NRC Research Press

ARTICLE

Phosphonate-functionalized heteroleptic ruthenium(II) bis(2,2′:6′,2″-terpyridine) complexes

Edwin C. Constable, Catherine E. Housecroft, Markéta Šmídková, and Jennifer A. Zampese

Abstract: The heteroleptic complexes [Ru(**1**)(**4**)][PF_6]$_2$, [Ru(**2**)(**4**)][PF_6]$_2$, [Ru(Phtpy)(**4**)][PF_6]$_2$, and [Ru(pytpy)(**4**)][PF_6]$_2$ (Phtpy = 4′-phenyl-2,2′:6′,2″-terpyridine, pytpy = 4′-(4-pyridyl)-2,2′:6′,2″-terpyridine, **1** and **2** = 4-methyl ester substituted derivatives of Phtpy and pytpy, **4** = ethyl 2,2′:6′,2″-terpyridine-4′-phosphonate) have been prepared. The single crystal structure of ligand **1** (**1** = methyl 4-carboxy-4′-phenyl-2,2′:6′,2″-terpyridine) is reported. The introduction of the 4-methyl ester group causes a small red shift in the MLCT band of the ruthenium(II) complexes and a small shift to a more positive potential for the Ru^{2+}/Ru^{3+} couple. The new complexes should serve as a useful starting point for development of ruthenium(II) dyes suited for sensitization of p-type semiconductors.

Key words: ruthenium, phosphonate functionalization, crystal structure, 2,2′:6′,2″-terpyridine, absorption spectroscopy, electrochemistry.

Résumé : Les complexes hétéroleptiques [Ru(**1**)(**4**)][PF_6]$_2$, [Ru(**2**)(**4**)][PF_6]$_2$, [Ru(Phtpy)(**4**)][PF_6]$_2$ et [Ru(pytpy)(**4**)][PF_6]$_2$ (Phtpy = 4′-phényl-2,2′:6′,2″-terpyridine, pytpy = 4′-(4-pyridyl)-2,2′:6′,2″-terpyridine, **1** et **2** = dérivés de la Phtpy et de la pytpy substitués par le 4-méthylester, **4** = éthyl 2,2′:6′,2″-terpyridine-4′-phosphonate) ont été préparés. La structure monocristalline du ligand **1** (**1** = méthyl 4-carboxy-4′-phényl-2,2′:6′,2″-terpyridine) est décrite dans le présent article. L'introduction du groupement 4-méthylester entraîne un décalage vers le rouge du spectre de transfert de charge du ligand au métal des complexes de ruthenium(II) et un léger décalage vers des potentiels plus positifs en ce qui concerne le couple Ru^{2+}/Ru^{3+}. Les nouveaux complexes devraient servir de points de départ au développement de colorants à base de ruthenium(II) conçus pour la sensibilisation des semicondicteurs de type p. [Traduit par la Rédaction]

Mots-clés : ruthenium, fonctionnalisation par un phosphonate, structure crystalline, 2,2′:6′,2″-terpyridine, spectroscopie d'absorption, électrochimie.

Introduction

The {Ru(tpy)$_2$} chromophore (tpy = 2,2′:6′,2″-terpyridine) is one of the most extensively studied domains[1] within metal oligopyridine coordination chemistry. Tuning the photophysical and electrochemical properties of {Ru(tpy)$_2$}-containing complexes is readily achieved through functionalization of the ligand. In particular, the Kröhnke methodology[2] is a facile means of introducing a wide variety of substituents into the 4′-position of tpy. Although at room temperature in solution, [Ru(tpy)$_2$]$^{2+}$ is essentially nonemissive,[3] judicious choice of electron-donating or accepting substituents can lead to significant enhancement of emission properties.[4]

Among the many areas in which ruthenium(II) complexes containing tpy-derived ligands have found a practical niche is that of the Grätzel solar cell.[5] Our own interests in the development of sensitizers for the photoanode in dye-sensitized solar cells have moved in the direction of earth-abundant metals, in particular copper.[6] Although photon-to-power conversion efficiencies reaching 3.77%[7] have been achieved with a copper(I) sensitizer anchored to the n-type semiconductor (TiO_2) comprising the photoanode, this is significantly lower than those attained by state-of-the-art ruthenium(II) dyes (>10%).[8] One strategy for improving performance is to harvest photons at both electrodes, but this requires different dyes suited for interaction with either the photoanode (n-type semiconductor) or the photocathode (p-type) in a so-called tandem cell.[9] In a tandem dye-sensitized solar cell, the photocathode functions in an inverse mode with respect to the photoanode, with excitation of the dye being followed by rapid hole injection into the p-type semiconductor (e.g., NiO). Organic donor–acceptor molecules are popular choices for photocathode sensitizers.[10] Excitation of the sensitizer leaves a hole in the original HOMO of the dye into which an electron is transferred from the valence band of the p-type semiconductor. Thus, the HOMO/LUMO requirements of a p-type sensitizer are the reverse of those of an n-type dye. It has been demonstrated that [Ru(bpy)$_2$(N^N)]$^{2+}$ (bpy = 2,2′-bipyridine, N^N = bipyridine-based anchoring ligand) complexes sensitize NiO photocathodes and both CO_2H and $PO(OH)_2$ anchors adsorb onto NiO.[11] Ruthenium(II) complexes containing cyclometalated ligands and related to the archetypal [Ru(bpy)$_2$(ppy)]$^+$[12,13] (Hppy = 2-phenylpyridine) are also promising candidates for NiO sensitization.[14,15]

Low-level MO calculations indicate that the HOMO of [Ru(tpy)(4′-$(HO)_2$OPtpy)]$^{2+}$ type complexes (4′-$(HO)_2$OPtpy = 2,2′:6′,2″-terpyridine-4′-phosphonic acid) may be localized on the phosphonic acid anchoring unit. We have therefore undertaken a preliminary investigation of several complexes of this type with the aim of providing a starting point for the development of dyes for p-type

Received 4 February 2014. Accepted 11 March 2014.

E.C. Constable, C.E. Housecroft, M. Šmídková, and J.A. Zampese. Department of Chemistry, University of Basel, Spitalstrasse 51, CH-4056 Basel, Switzerland.

Corresponding author: Catherine E. Housecroft (e-mail: catherine.housecroft@unibas.ch).

This article is part of a Special Issue dedicated to Professor Barry Lever in recognition of his contributions to inorganic chemistry across Canada and beyond.

This paper is dedicated to our colleague Barry Lever whose contributions to inorganic chemistry have extended over a long and distinguished career.

semiconductors. The ancillary ligands **1** and **2** (Scheme 1) contain an ester functionality that provides a site for variable functionalization, for example, through transesterification.

Experimental

General

^{1}H and ^{13}C NMR spectra were recorded at 295 K on Bruker Avance III-400 or III-500 NMR spectrometers (chemical shifts with respect to residual solvent peaks and δ(TMS) = 0 ppm). Solution electronic absorption and emission spectra were measured, respectively, using an Agilent 8453 spectrophotometer and Shimadzu 5301PC spectrofluorophotometer. Solution quantum yields were measured using a Hamamatsu absolute PL quantum yield spectrometer C11347 Quantaurus_QY. A Shimadzu 8400S spectrometer was used to record FT-IR spectra (all solid samples using a Golden Gate accessory). Electrospray ionization (ESI) mass spectra and high-resolution ESI mass spectra were recorded on Bruker esquire 3000^{plus} and Bruker maXis 4G mass spectrometers. Electrochemical measurements were carried out using cyclic voltammetry and were recorded using a CH Instruments 900B potentiostat with glassy carbon working and platinum auxiliary electrodes; a silver wire was used as a pseudo-reference electrode. The solvent was HPLC-grade MeCN and 0.05 mol L^{-1} [^{n}Bu$_4$N][PF$_6$] was used as supporting electrolyte. All solutions were degassed with argon, and Cp_2Fe was used as an internal reference. A Biotage Initiator 8 reactor was used for reactions under microwave conditions. Fluka silica 60 was used for column chromatography.

The compounds (*E*)-1-(pyridin-2-yl)-3-(pyridin-4-yl)prop-2-en-1-one,[16] (*E*)-3-phenyl-1-(pyridin-2-yl)prop-2-en-1-one,[17] 1-(2-(4-(methoxycarbonyl) pyridin-2-yl)-2-oxoethyl)pyridine-1-ium iodide,[16] Phtpy,[17] pytpy,[18] and 4′-F$_3$CSO$_3$-2,2′:6′,2″-terpyridine[19] were prepared according to published methods (Phtpy = 4′-phenyl-2,2′:6′,2″-terpyridine, pytpy = 4′-(4-pyridyl)-2,2′:6′,2″-terpyridine). $RuCl_3{\cdot}3H_2O$ was purchased from OXKEM.

Compound 1

Ammonium acetate (9.60 g, 124.68 mmol) was dissolved in MeOH (110 mL). (*E*)-3-Phenyl-1-(pyridin-2-yl)prop-2-en-1-one (1.00 g, 4.76 mmol) and 1-(2-(4-(methoxycarbonyl)pyridin-2-yl)-2-oxoethyl) pyridine-1-ium iodide (2.21 g, 5.71 mmol) were added and the brown solution was heated at reflux for 16 h, during which time a brown precipitate formed. The reaction mixture was then cooled to room temperature and left to stand overnight in a freezer. The brown precipitate was collected on a glass frit, washed with cold MeOH, and dried in air. Compound **1** was isolated as a pale brown powder (0.56 g, 1.53 mmol, 33%); mp 197–198 °C. ^{1}H NMR (500 MHz, $CDCl_3$) δ (ppm): 9.16 (dd, *J* = 1.7, 0.9 Hz, 1H, H^{D3}), 8.86 (dd, *J* = 5.0, 0.9 Hz, 1H, H^{D6}), 8.78 (d, *J* = 1.7 Hz, 1H, H^{B3}), 8.75 (d, *J* = 1.7 Hz, 1H, H^{B5}), 8.74 (ddd, *J* = 4.7, 1.9, 1.0 Hz, 1H, H^{A6}), 8.72 (dt, *J* = 7.9, 1.1 Hz, 1H, H^{A3}), 7.90 (m, 4H, H$^{A4+C2+D5}$), 7.52 (m, 2H, H^{C3}), 7.47 (m, 1H, H^{C4}), 7.37 (ddd, *J* = 7.5, 4.8, 1.2 Hz, 1H, H^{A5}), 4.04 (s, 3H, H^{OMe}). ^{13}C{^{1}H} NMR (126 MHz, $CDCl_3$) δ (ppm): 166.1 (C$^{C=O}$), 157.6 (C^{D2}), 156.2 (C^{A2}), 156.1 (C^{B2}), 155.3 (C^{B6}), 150.6 (C^{B4}), 150.0 (C^{D6}), 149.2 (C^{A6}), 138.5 (C^{C1}), 138.4 (C^{D4}), 137.2 (C^{A4}), 129.3 (C^{C4}), 129.1 (C^{C3}), 127.5 (C^{C2}), 124.1 (C^{A5}), 122.9 (C^{D5}), 121.7 (C^{A3}), 120.8 (C^{D3}), 119.5 (C^{B5}), 119.3 (C^{B3}), 52.9 (C^{OMe}). ESI-MS (MeOH/$CHCl_3$): *m*/*z* 390.0 [M+Na]$^+$ (calcd. 390.1), 368.0 [M+H]$^+$ (base peak, calcd. 368.1). IR (solid, *ν* (cm^{-1})): 3051 (w), 2969 (w), 1723 (s), 1583 (m), 1548 (m), 1467 (w), 1432 (m), 1378 (s), 1268 (s), 1218 (s), 1132 (w), 1099 (w), 989 (m), 887 (w), 800 (m), 775 (m), 764 (s), 754 (s), 731 (s), 707 (s), 694 (s), 681 (s), 662 (s), 620 (s), 517 (s). UV/VIS λ (nm) (CH_3CN, 4.44 × 10^{-5} mol dm^{-3}) (*ε* (dm^3 mol^{-1} cm^{-1})): 253 (35 000), 276 sh (27 000), 310 sh (13 000). Found: C 74.41, H 4.67, N 11.22; $C_{23}H_{17}N_3O_2{\cdot}0.25H_2O$ requires C 74.28, H 4.74, N 11.30%.

Compound 2

Ammonium acetate (13 g, 160 mmol) was dissolved in MeOH (150 mL). (*E*)-1-(Pyridin-2-yl)-3-(pyridin-4-yl)prop-2-en-1-one (0.92 g, 4.38 mmol) and 1-(2-(4-(methoxycarbonyl)pyridin-2-yl)-2-oxoethyl) pyridine-1-ium iodide (2.01 g, 5.25 mmol) were added and the brown suspension was heated at reflux for 7 h; the solids slowly dissolved. The white precipitate that formed was collected on a glass frit, washed with cold MeOH and Et_2O, and dried in air. Compound **2** was isolated as a white powder (1.43 g, 3.88 mmol, 89%); mp 216–217 °C. ^{1}H NMR (500 MHz, $CDCl_3$) δ (ppm): 9.15 (dd, *J* = 1.6, 0.9 Hz, 1H, H^{D3}), 8.86 (dd, *J* = 5.0, 0.9 Hz, 1H, H^{D6}), 8.78 (d, *J* = 1.7 Hz, 1H, H^{B3}), 8.76 (m, 3H, H^{C2+B5}), 8.72 (m, 2H, H^{A6+A3}), 7.92 (m, 2H, H^{A4+D5}), 7.80 (dd, *J* = 4.5, 1.7 Hz, 2H, H^{C3}), 7.39 (ddd, *J* = 7.5, 4.8, 1.3 Hz, 1H, H^{A5}), 4.04 (s, 3H, H^{OMe}). ^{13}C{^{1}H} NMR (126 MHz, $CDCl_3$) δ (ppm): 165.9 (C$^{C=O}$), 156.9 (C^{D2}), 156.7 (C^{B2}), 155.6 (C^{B6}), 155.5 (C^{A2}), 150.6 (C^{C2}), 150.0 (C^{D6}), 149.3 (C^{A6}), 147.6 (C^{B4}), 145.9 (C^{C4}), 138.5 (C^{D4}), 137.2 (C^{A4}), 124.3 (C^{A5}), 123.2 (C^{D5}), 121.7 (C^{C3}), 121.6 (C^{A3}), 120.7 (C^{D3}), 119.1 (C^{B3}), 118.9 (C^{B5}), 53.0 (C^{OMe}). ESI-MS (MeOH/$CHCl_3$): *m*/*z* 391.1 [M+Na]$^+$ (base peak, calcd. 391.1), 369.2 [M+H]$^+$ (calcd. 369.1). IR (solid, *ν* (cm^{-1})): 3020 (w), 2961 (w), 1731 (s), 1583 (m), 1559 (m), 1538 (m), 1533 (m), 1475 (m), 1436 (m), 1378 (m), 1309 (w), 1292 (w), 1270 (m), 1263 (w), 1218 (m), 1211 (m), 1130 (w), 973 (w), 895 (w), 821 (m), 795 (s), 770 (s), 736 (w), 682 (m), 669 (m), 660 (m), 618 (m), 533 (m). UV/VIS λ (nm) (*ε* (dm^3 mol^{-1} cm^{-1})) (CH_3CN, 4.22 × 10^{-5} mol dm^{-3}): 242 (33000), 281 (16000), 316 sh (10000). Found: C 70.96, H 4.44, N 15.19; $C_{22}H_{16}N_4O_2{\cdot}0.25H_2O$ requires C 70.86, H 4.46, N 15.02%.

Compound 3

4′-F$_3$CSO$_3$-2,2′:6′,2″-Terpyridine (0.80 g, 2.10 mmol) and [Pd(PPh$_3$)$_4$] (0.24 g, 0.21 mmol) were suspended in MeCN (17 mL) in a microwave vial (20 mL) and then NEt_3 (0.38 g, 3.78 mmol) and diethyl phosphite (0.49 g, 3.57 mmol) were added. The brown suspension was heated in a microwave reactor (140 °C, 30 min) and then allowed to cool to room temperature. The reaction mixture was diluted with toluene and washed with aqueous NH_4OH (32%) and water. The organic layer was dried over $MgSO_4$, filtered, and the solvent removed in vacuo. The crude brown solid was purified by flash column chromatography (SiO_2), first eluting with CH_2Cl_2 to remove Ph_3PO and then with CH_2Cl_2–MeOH (98:2). Com-

Scheme 1. Structures of ligands **1–4** and of Phtpy and pytpy, with atom numbering used for NMR spectroscopic assignments; when R = H, ring A = ring D.

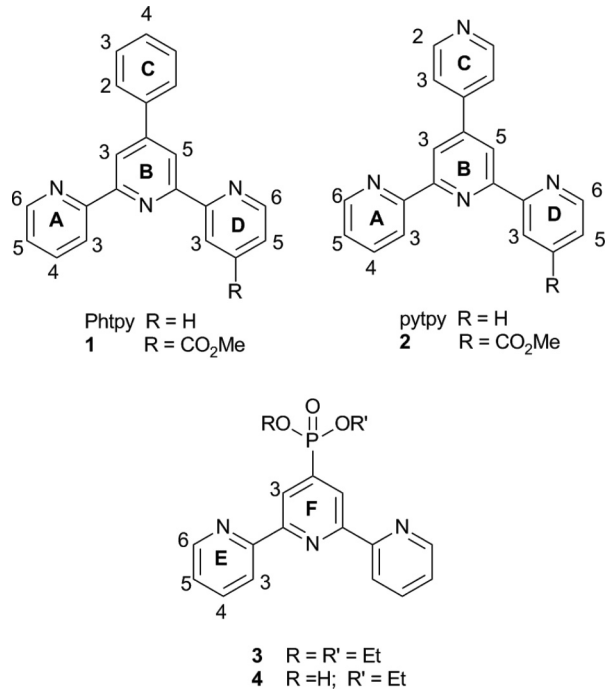

pound **3** was isolated as a pale brown solid (0.65 g, 1.76 mmol, 84%). The NMR spectroscopic data matched those published.[20]

[Ru(3)Cl$_3$]

Compound **3** (0.60 g, 1.63 mmol) and $RuCl_3{\cdot}3H_2O$ (0.43 g, 1.63 mmol) were suspended in EtOH (200 mL) and the reaction mixture was heated at reflux for 3.5 h. The brown solid that formed was separated by filtration, washed with cold EtOH and Et_2O, and dried in air, yielding a red-brown powder (0.83 g, 1.44 mmol, 88%). The product was used for the next step without further purification and characterization.

[Ru(Phtpy)(4)][PF$_6$]$_2$

Phtpy (64 mg, 0.21 mmol) and [Ru(**3**)Cl$_3$] (119 mg, 0.21 mmol) were suspended in dry EtOH (3.5 mL) in a microwave reactor vial. *N*-Ethylmorpholine (three drops) was added and the reaction mixture was heated in a microwave reactor at 140 °C for 15 min. The dark red solution was poured into aqueous NH_4PF_6 (250 mL), yielding a red precipitate that was collected on Celite and washed with cold water (250 mL) and Et_2O (20 mL). The residue was redissolved in CH_3CN and then solvent removed in vacuo to give a dark red solid. This was purified by column chromatography (SiO_2, eluted with CH_3CN – saturated aqueous KNO_3 – water 7:1:0.5 by volume). The first red band was collected, aqueous NH_4PF_6 added, and solvent evaporated until a red precipitate formed. This was collected on Celite and washed thoroughly with cold water (250 mL), cold EtOH (15 mL), and Et_2O (15 mL). The residue was redissolved in CH_3CN and solvent removed in vacuo. [Ru(Phtpy)(**4**)][PF$_6$]$_2$ was isolated as a red powder (200 mg, 0.192 mmol, 93%). ^{1}H NMR (400 MHz, CD_3CN) δ (ppm): 9.06 (d, J_{PH} = 11 Hz, 2H, H^{F3}), 8.99 (s, 2H, H^{B3}), 8.68 (m, 4H, H^{A3+E3}), 8.20 (m, 2H, H^{C2}), 7.90 (m, 4H, H^{A4+E4}), 7.76 (m, 2H, H^{C3}), 7.68 (m, 1H, H^{C4}), 7.39 (m, 4H, H^{A6+E6}), 7.15 (m, 4H, H^{A5+E5}), 4.05 (m, 2H, H$^{CH2(Et)}$), 1.31 (t, *J* = 7.0 Hz, 3H, H$^{CH3(Et)}$). ^{13}C{^{1}H} NMR (126 MHz, CD_3CN) δ (ppm): 159.3 (C^{E2}), 158.8 (C^{A2}), 156.2 (C^{B2}), 155.7 (d, J_{PC} = 12 Hz, C^{F2}), 153.7 (C$^{A6/E6}$), 153.3 (C$^{A6/E6}$), 149.2 (C^{B4}), 139.0 (C^{A4+E4}), 137.9 (C^{C1}), 131.3 (C^{C4}), 130.6 (C^{C3}), 128.7 (C^{C2}), 128.5 (C$^{A5/E5}$), 128.2 (C$^{A5/E5}$), 126.4 (d, J_{PC} = 20 Hz, C^{F3}), 125.6 (C$^{A3/E3}$), 125.4 (C$^{A3/E3}$), 122.5 (C^{B3}), 61.8 (C$^{CH2(Et)}$), 17.5 (C$^{CH3(Et)}$) (C^{F4} not resolved). IR (solid, *ν* (cm^{-1})): 3315 (br m), 1662 (w), 1605 (w), 1542 (w), 1473 (w), 1412 (m), 1392 (m), 1345 (m), 1289 (w), 1209 (m), 1162 (w), 1140 (m), 1078 (m), 1034 (m), 962 (w), 898 (w), 826 (s), 791 (s), 764 (s), 733 (m), 689 (s), 664 (m), 603 (m). ESI-MS (MeCN): *m*/*z* 751.4 [M – H – 2PF$_6$]$^+$ (100%, calcd. 751.1). HR ESI-MS *m*/*z*: 376.0621 [M – 2PF$_6$]$^{2+}$ (base peak, calcd. 376.0619), 751.1172 [M – H – 2PF$_6$]$^+$ (calcd. 751.1165). UV/VIS λ (nm) (MeCN, 2.88 × 10^{-5} mol dm^{-3}) (*ε* (dm^3 mol^{-1} cm^{-1})): 274 (59000), 280 sh (54500), 310 (63000), 330 sh (34000), 485 (23000). Emission (MeCN, 3 × 10^{-5} mol dm^{-3}, λ_{ex} = 485 nm): λ_{em} = 647 nm. Satisfactory elemental analysis could not be obtained (see text).

[Ru(pytpy)(4)][PF$_6$]$_2$

The method was as for [Ru(Phtpy)(**4**)][PF$_6$]$_2$ starting with pytpy (160 mg, 0.52 mmol) and [Ru(**3**)Cl$_3$] (300 mg, 0.52 mmol). [Ru(pytpy)(**4**)][PF$_6$]$_2$ was isolated as a red powder (130 mg, 0.125 mmol, 24%). ^{1}H NMR (500 MHz, CD_3CN) δ (ppm): 9.05 (d, J_{PH} = 11 Hz, 2H, H^{F3}), 9.03 (s, 1H, H^{B3}), 8.95 (m, 2H, H^{C2}), 8.64 (d, *J* = 7.9 Hz, 2H, H$^{A3/E3}$), 8.61 (d, *J* = 8.1 Hz, 2H, H$^{A3/E3}$), 8.12 (m, 2H, H^{C3}), 7.94 (m, 2H, H$^{A4/E4}$), 7.88 (m, 2H, H$^{A4/E4}$), 7.42 (d, *J* = 6.7 Hz, 2H, H$^{A6/E6}$), 7.35 (d, *J* = 6.7 Hz, 2H, H^{E6}), 7.18 (m, 2H, H$^{A5/E5}$), 7.15 (m, 2H, H$^{A5/E5}$), 4.05 (m, 2H, H$^{CH2(Et)}$), 1.32 (t, *J* = 6.8 Hz, 3H, H$^{CH3(Et)}$). ^{13}C{^{1}H} NMR (126 MHz, CD_3CN) δ (ppm): 158.7 (C^{E2}), 158.5 (C^{A2}), 158.0 (C^{F2}), 157.0 (C^{B2}), 153.8 (C$^{A6/E6}$), 153.7 (C$^{A6/E6}$), 151.5 (C^{C2}), 145.3 (C^{B4+C4}), 139.3 (C^{A4+E4}), 128.8 (C$^{A5/E5}$), 128.6 (C$^{A5/E5}$), 126.2 (d, J_{PC} ≈ 20 Hz, C^{F3}), 126.1 (C$^{A3/E3}$), 126.0 (C$^{A3/E3}$), 123.2 (C^{B3}), 123.1 (C^{C3}), 63.2 (C$^{CH2(Et)}$), 17.2 (C$^{CH3(Et)}$) (C^{F4} not resolved). IR (solid, *ν* (cm^{-1})): 3350 (br s), 1660 (w), 1599 (s), 1532 (w), 1475 (m), 1394 (m), 1352 (w), 1291 (w), 1202 (s), 1166 (w), 1075 (m), 1069 (m), 1038 (m), 1028 (s), 942 (m), 844 (s), 826 (s), 818 (s), 784 (m), 776 (m), 745 (m). ESI-MS (CH_3CN): *m*/*z* 376.5 [M – 2PF$_6$]$^{2+}$ (calcd. 376.6). HR ESI-MS *m*/*z*: 376.5600 [M – 2PF$_6$]$^{2+}$ (base peak, calcd. 376.5595), 752.1135 [M – H – 2PF$_6$]$^+$ (calcd. 752.1117). UV/VIS λ (nm) (CH_3CN, 1 × 10^{-5} mol dm^{-3}) (*ε* dm^3 mol^{-1} cm^{-1})): 273 (54700), 282 sh (42000), 311 (50300), 331 sh (33000), 486 (21000). Emission (CH_3CN, 3.84 × 10^{-5} mol dm^{-3}, λ_{ex} = 486 nm): λ_{em} = 704 nm. Found: C 42.94, H 3.76, N 10.33; $C_{37}H_{30}F_{12}N_7O_3P_3Ru{\cdot}H_2O{\cdot}1.5CH_3CN$(1122.60) requires C 42.81, H 3.28, N 10.16%.

[Ru(1)(4)][PF$_6$]$_2$

The method was as for [Ru(Phtpy)(**4**)][PF$_6$]$_2$ starting with **1** (71 mg, 0.19 mmol) and [Ru(**3**)Cl$_3$] (112 mg, 0.19 mmol). [Ru(**1**)(**4**)][PF$_6$]$_2$ was isolated as a red powder (177 mg, 0.161 mmol, 83%). ^{1}H NMR (400 MHz, CD_3CN) δ (ppm): 9.15 (d, *J* = 1.4 Hz, 1H, H$^{B3/B5}$), 9.12 (d, J_{PH} = 10. Hz, 2H, H^{F3}), 9.08 (d, J = 1.2 Hz, 1H, H^{D3}), 9.05 (d, *J* = 1.4 Hz, 1H, H$^{B3/B5}$), 8.72 (d, *J* = 8.2 Hz, 2H, H^{E3}), 8.66 (d, *J* = 7.9 Hz, 1H, H^{A3}), 8.24 (m, 2H, H^{C2}), 7.94 (td, *J* = 7.9, 1.5 Hz, 1H, H^{A4}), 7.89 (td, *J* = 7.9, 1.5 Hz, 2H, H^{E4}), 7.77 (m, 2H, H^{C3}), 7.69 (m, 1H, H^{C4}), 7.63 (d, *J* = 5.8 Hz, 1H, H^{D6}), 7.56 (dd, *J* = 5.8, 1.8 Hz, 1H, H^{D5}), 7.44 (d, *J* = 5.5 Hz, 1H, H^{A6}), 7.39 (dd, *J* = 5.6, 1.4 Hz, 2H, H^{E6}), 7.18 (m, 1H, H^{A5}), 7.13 (ddd, *J* = 7.7, 5.6, 1.3 Hz, 2H, H^{E5}), 4.07 (m, 2H, H$^{CH2(Et)}$), 3.90 (s, 3H, H^{OMe}), 1.29 (t, *J* = 7.0 Hz, 3H, H$^{CH3(Et)}$). ^{13}C{^{1}H} NMR (126 MHz, CD_3CN) δ (ppm): 165.0 (C$^{C=O}$), 160.6 (C^{D2}), 159.5 (C^{E2}), 159.0 (C^{A2}), 156.4 (C^{B2}), 156.0 (C^{B6}), 154.7 (C^{D6}), 155.6 (d, J_{PC} = 14 Hz, C^{F2}), 153.7 (C^{A6}), 153.3 (C^{E6}), 149.4 (C^{B4}), 139.4 (C^{D4}), 139.2 (C^{A4+E4}), 137.6 (C^{C1}), 131.4 (C^{C4}), 130.6 (C^{C3}), 129.0 (C^{C2}), 128.6 (C^{A5+E5}), 128.2 (C^{D5}), 127.6 (d, J_{PC} = 10 Hz, C^{F3}), 126.8 (C^{E3}), 126.5 (C^{A3}), 125.1 (C^{D3}), 124.0 (C$^{B3/B5}$), 123.7 (C$^{B3/B5}$), 62.1 (C$^{CH2(Et)}$), 54.3 (C^{OMe}), 17.5 (C$^{CH3(Et)}$) (C^{F4} not resolved). IR (solid, *ν* (cm^{-1})): 3347 (br m), 1722 (w), 1605 (w), 1363 (m), 1268 (w), 1165 (w), 1137 (w), 1075 (w), 1032 (w), 945 (w), 825 (s), 787 (m), 767 (m), 700 (w), 607 (w). ESI-MS (CH_3CN): *m*/*z* 809.5 [M – H – 2PF$_6$]$^+$ (base peak, calcd. 809.1). HR ESI-MS *m*/*z*: 405.0654 [M – 2PF$_6$]$^{2+}$ (base peak, calcd. 405.0647), 809.1233 [M – H – 2PF$_6$]$^+$ (calcd. 809.1220). UV/VIS λ (nm): (CH_3CN, 3.6 × 10^{-5} mol dm^{-3}) (*ε* (dm^3 mol^{-1} cm^{-1})): 274 (56 000), 285 (51 500), 309 (57 000), 330 sh (41500), 491 (20 000). Satisfactory elemental analysis was not obtained (see text).

[Ru(2)(4)][PF$_6$]$_2$

The method was as for [Ru(Phtpy)(**4**)][PF$_6$]$_2$ starting with **2** (50 mg, 0.14 mmol) and [Ru(**3**)Cl$_3$] (78 mg, 0.14 mmol). [Ru(**2**)(**4**)][PF$_6$]$_2$ was isolated as a red powder (35 mg, 0.032 mmol, 23%). ^{1}H NMR (500 MHz, CD_3CN) δ (ppm): 9.23 (d, J_{PH} = 11.5 Hz, 2H, H^{F3}) overlapping with 9.14 (d, *J* = 1.5 Hz, 1H, H$^{B3/B5}$), 9.12 (d, *J* = 1.3 Hz, 1H, H$^{B3/B5}$), 9.09 (d, *J* = 1.4 Hz, 1H, H^{D3}), 8.98 (m, 2H, H^{C2}), 8.77 (m, 3H, H^{A3+E3}), 8.19 (m, 2H, H^{C3}), 7.98 (td, *J* = 8.1, 1.4 Hz, 1H, H^{A4}), 7.92 (td, *J* = 7.9, 1.5 Hz, 2H, H^{E4}), 7.61 (m, 2H, H^{D5+D6}), 7.46 (d, *J* = 5.6 Hz, 1H, H^{A6}), 7.38 (dd, *J* = 5.7, 1.3 Hz, 2H, H^{E6}), 7.21 (m, 1H, H^{A5}), 7.16 (ddd, *J* = 7.2, 5.6, 1.2 Hz, 2H, H^{E5}), 4.27 (m, 2H, H$^{CH2(Et)}$), 3.91 (s, 3H, H^{OMe}), 1.41 (t, *J* = 6.9 Hz, 3H, H$^{CH3(Et)}$). ^{13}C{^{1}H} NMR (126 MHz, CD_3CN) δ (ppm): 164.3 (C$^{C=O}$), 160.1 (C^{D2}), 159.5 (C^{F2}), 159.3 (C^{E2}), 158.8 (C^{A2}), 157.1 (C^{B2}), 156.5 (C^{B6}), 154.8 (C^{D6}), 153.7 (C^{A6}), 153.4 (C^{E6}), 151.7 (C^{C2}), 146.4 (C^{B4}), 145.2 (C^{C4}), 139.4 (C^{A4}), 139.3 (C^{E4}), 128.6 (C^{A5}), 128.5 (C^{E5}), 127.3 (C^{D5}), 126.4 (d, J_{PC} ≈ 10 Hz, C^{F3}), 126.0 (C^{E3}), 125.7 (C^{A3}), 124.4 (C$^{B3/B5}$), 123.3 (C$^{B3/B5}$), 123.0 (C^{D3}), 123.1 (C^{C3}), 62.6 (C$^{CH2(Et)}$), 53.8 (C^{OMe}), 16.9 (C$^{CH3(Et)}$) (C^{F4} and C^{D4} not resolved). IR (solid, *ν* (cm^{-1})): 3211 (br s), 1729 (m), 1635 (w), 1600 (w), 1475 (w), 1409 (m), 1344 (w), 1313 (m), 1268 (m), 1235 (m), 1165 (m), 1138 (m), 1076 (m), 1030 (m), 950 (m), 826 (s), 786 (s), 753 (m), 688 (m), 652 (m), 605 (m). ESI-MS (MeCN): *m*/*z* 405.6 [M – 2PF$_6$]$^{2+}$ (calcd. 405.6). HR ESI-MS *m*/*z*: 405.5628 [M – 2PF$_6$]$^{2+}$ (base peak, calcd. 405.5623), 810.1187 [M – H – 2PF$_6$]$^+$ (calcd. 810.1173). UV/VIS λ (nm) (CH_3CN, 3.63 × 10^{-5} mol dm^{-3}) (*ε* (dm^3 mol^{-1} cm^{-1})): 274 (51 000), 284 sh (43 500), 308 (45 000), 330 sh (37 000), 491 (18 500). Satisfactory elemental analysis could not be obtained (see text).

Crystal structure determination of 1

Data were collected on a Bruker-Nonius Kappa APEX diffractometer; data reduction, solution, and refinement used APEX2[21]

and SHELX13.[22] Absorption correction was made using the program "sadabs" as part of the "scale" package in AEPX2 software.[21] The ORTEP plot was produced with Mercury v. 3.0,[23,24] which was also used for structure analysis. $C_{23}H_{17}N_3O_2$, M = 367.40, colorless plate, crystal dimensions 0.25 mm × 0.13 mm × 0.03 mm, monoclinic, space group $P2_1/c$, a = 9.9644(9), b = 9.0359(8), c = 20.0424(17) Å, β = 96.975(6)°, U = 1791.2(3) Å^3, Z = 4, D_c = 1.362 Mg m^{-3}, μ(Cu-Kα) = 8.224 mm^{-1}, T = 123 K. Total 18 887 reflections, 3181 unique, R_{int} = 0.0428. Refinement of 2763 reflections (254 parameters) with $I > 2\sigma(I)$ converged at final R_1 = 0.0378 (R_1 all data = 0.0439), wR_2 = 0.1009 (wR_2 all data = 0.1048), goodness-of-fit = 1.064.

Results and discussion

Synthesis and characterization of ligands 1 and 2

Compounds **1** and **2** (Scheme 1) are the 4′-phenyl and 4′-(4-pyridyl) analogues of 4′-tolyl-2,2′:6′,2″-terpyridine, the preparation and homoleptic ruthenium(II) complex of which were reported a decade ago by Potvin and co-worker.[25] Scheme 2 shows the Kröhnke synthesis of **1** and **2**, which yielded the compounds in 33% and 89%, respectively, as white solids. In the electrospray mass spectrum of **1**, the base peak (m/z = 338.0) arises from the $[M + H]^+$ ion, and a lower intensity peak at m/z = 390.0 was assigned to $[M + Na]^+$. Corresponding peaks at m/z 369.2 and 391.1 in the mass spectrum of **2** were also observed. The ^{1}H and ^{13}C NMR spectra of **1** and **2** were fully assigned with COSY, HMQC, and HMBC techniques and were consistent with the inequivalence of the outer pyridine rings of the tpy domain (Scheme 1) and the presence of the ester group.

Single crystals of **1** were grown by slow evaporation from a $CHCl_3$ solution of the compound and the structure (Fig. 1) was confirmed by X-ray diffraction. Important bond parameters are given in the figure caption. The tpy unit adopts a *trans*,*trans*-conformation, which is expected for a nonprotonated ligand. The tpy domain is essentially planar (the angles between the least squares planes through the rings containing N1/N2 and N2/N3 = 5.5° and 4.5°); the phenyl ring is twisted 27.6° with respect to the pyridine ring to which it is attached, consistent with minimizing H···H repulsions between the two rings. The dominant packing interactions are (1) face-to-face π-stacking of tpy domains across inversion centres, (2) $H_{methyl}\cdots N_{pyridine}$ contacts (H23A···N1^i = 2.98, H23B···N1^i = 2.81 Å, symmetry code i = 1 + x, 1 + y, z), and (3) $N_{pyridine}\cdots$HC contacts (N3···H3A^{ii}–C3^{ii} = 2.57 Å, symmetry code ii = x, 3/2 – y, 1/2 + z).

The diethylphosphonate-functionalized ligand **3** has previously been reported by Grätzel and co-workers.[20] The literature synthesis (which gives **3** in 72.3% yield) involves the $[Pd(PPh_3)_4]$ catalysed reaction of 4′-bromo-2,2′:6′,2″-terpyridine with diethyl phosphite in NEt_3 (95 °C for 3 h) followed by dissolution of the mixture in MeOH and chromatographic workup. We adopted the more convenient strategy shown in Scheme 2. The 4′-triflate-functionalized tpy was readily prepared according to the route described by Potts et al.,[19] and diethylphosphonate for triflate substitution occurs under microwave conditions to give **3** in 84% yield (Scheme 3). The NMR spectroscopic data for **3** were consistent with those published.[20]

Synthesis and characterization of heteroleptic ruthenium(II) complexes

The heteroleptic complexes discussed in this section are summarized in Scheme 4. Heteroleptic $[Ru(Xtpy)(Ytpy)]^{2+}$ complexes are typically prepared by first preparing an insoluble, paramagnetic ruthenium(III) complex $[Ru(Xtpy)Cl_3]$ and treating this crude material with Ytpy in the presence of *N*-ethylmorpholine, which acts as a reducing agent.[26] The precursor for the formation of the new ruthenium(II) complexes was $[Ru(\mathbf{3})Cl_3]$, prepared by reaction of $RuCl_3.3H_2O$ with compound **3** in MeOH under reflux. $[Ru(\mathbf{3})Cl_3]$ was isolated as a brown solid.

Model compounds containing Phtpy and pytpy (Scheme 1) were first prepared by reaction of $[Ru(\mathbf{3})Cl_3]$ with Phtpy and pytpy in the presence of *N*-ethylmorpholine. After anion exchange and chromatographic workup, followed by a second anion exchange (to remove $[NO_3]^-$ introduced from aqueous KNO_3 in the eluant), the ruthenium(II) salts were isolated as red solids. Electrospray mass spectrometic and NMR spectroscopic data were consistent with the isolated products being complexes of the monoester **4** (Scheme 2) rather than the diester **3**. Partial hydrolysis of **3** during synthesis of ruthenium(II) complexes is known to occur under conditions of high temperature reflux[20] or heating in DMF at 60 °C.[27] The second hydrolysis step to the phosphonic acid needs acidic conditions or treatment with Me_3SiBr. The ESI mass spectrum of $[Ru(Phtpy)(\mathbf{4})][PF_6]_2$ showed the base peak envelope at m/z 751.4 with an appropriate isotope pattern for the ion $[M - H - 2PF_6]^+$. The loss of H^+ is consistent with the presence of the acidic P–OH group. The high-resolution ESI (HR-ESI) mass spectrum was also recorded and peaks arising from $[M - H - 2PF_6]^+$ and $[M - 2PF_6]^{2+}$ confirmed the identity of $[Ru(Phtpy)(\mathbf{4})]^{2+}$. The HR-ESI mass spectrum of $[Ru(pytpy)(\mathbf{4})][PF_6]_2$ exhibited peak envelopes arising from the $[M - H - 2PF_6]^+$ and $[M - 2PF_6]^{2+}$ ions, and the latter was also observed in the ESI mass spectrum.

The ^{1}H and ^{13}C NMR spectra of CD_3CN solutions of $[Ru(Phtpy)(\mathbf{4})][PF_6]_2$ and $[Ru(pytpy)(\mathbf{4})][PF_6]_2$ were consistent with the presence of two tpy environments in each complex. A representative spectrum is shown in Fig. 2. Spectra were assigned using 2D methods (COSY, HMQC, and HMBC); 400 MHz ^{1}H spectra were routinely recorded for better resolution of signals and 500 MHz ^{1}H for 2D measurements. The most characteristic feature of the spectrum in Fig. 2 is the appearance of a singlet for protons H^{B3} (Phtpy ligand) and a doublet for the corresponding protons H^{F3} (ligand **4**) arising from ^{31}P–^{1}H coupling (11 Hz). For $[Ru(Phtpy)(\mathbf{4})][PF_6]_2$, signals at δ 4.05 and 1.31 ppm in the ^{1}H NMR spectrum and their relative integrals with respect to resonances in the aromatic region were consistent with the monoester **4**; in the ^{13}C NMR spectrum, corresponding signals at δ 61.8 and 17.5 ppm were observed.

The preparations of $[Ru(\mathbf{1})(\mathbf{4})][PF_6]_2$ and $[Ru(\mathbf{2})(\mathbf{4})][PF_6]_2$ were carried out in an analogous manner to those of $[Ru(Phtpy)(\mathbf{4})][PF_6]_2$ and $[Ru(pytpy)(\mathbf{4})][PF_6]_2$. The base peak in the ESI mass spectrum of $[Ru(\mathbf{1})(\mathbf{4})][PF_6]_2$ was assigned to $[M - H - 2PF_6]^+$; for $[Ru(\mathbf{2})(\mathbf{4})][PF_6]_2$, the main peak envelope arose from $[M - 2PF_6]^{2+}$. High-resolution ESI data showed peaks arising from $[M - 2PF_6]^{2+}$ and $[M - H - 2PF_6]^+$ for both complexes. The solution ^{1}H and ^{13}C NMR spectra (assigned by 2D methods) of $[Ru(\mathbf{1})(\mathbf{4})][PF_6]_2$ and $[Ru(\mathbf{2})(\mathbf{4})][PF_6]_2$ were consistent with the presence of the symmetrical ligand **4** and one asymmetrical ligand. Figure 3 shows part of the ^{1}H NMR spectrum of $[Ru(\mathbf{2})(\mathbf{4})][PF_6]_2$. The doublet for H^{F3} (J_{PH} = 11.5 Hz) overlaps with one of the two doublets (J_{HH} 1.3 or 1.5 Hz) arising from H^{B3} and H^{B5}. Pairs of signals for H^{E3}/H^{A3}, H^{E4}/H^{A4}, H^{E5}/H^{A5}, and H^{E6}/H^{A6} with relative integrals 2:1 appear for the unsubstituted pyridine rings in ligand **4** and for ligands **1** or **2**, respectively. The signal for H^{D3} (J_{HH} = 1.4 Hz) was distinguished from those of H^{B3} and H^{B5} by its COSY signature. The relative integrals for the signals for the ethyl groups in **4** in both complexes were consistent with the monoester.

Yields of $[Ru(Phtpy)(\mathbf{4})][PF_6]_2$ and $[Ru(\mathbf{1})(\mathbf{4})][PF_6]_2$ were >80%, but for the complexes containing pytpy, lower yields of approximately 25% were observed, due, in part, to formation of some of the N-protonated species. We noted changes in the ^{1}H NMR spectra that were consistent with protonation of samples in solution. Satisfactory elemental analysis could not always be obtained for the hexafluoridophosphate salts, probably due to small amounts of residual NH_4PF_6. Traces of $[NH_4]^+$ were seen in the ^{1}H NMR spectra (δ 6.02, $J(^{14}N^1H)$ = 53 Hz) of some batches of the complexes. X-ray-quality crystals of solvated $[Ru(pytpy)(\mathbf{4})][PF_6]_2$ were obtained, but only preliminary structural data could be obtained because of persistent twinning problems. However, these data were sufficient to confirm the presence of the monoester ligand **4** and the octahedral coordination environment of the rutheni-

Scheme 2. Synthetic route to ligands **1** and **2**. Conditions: (*i*) MeOH, reflux.

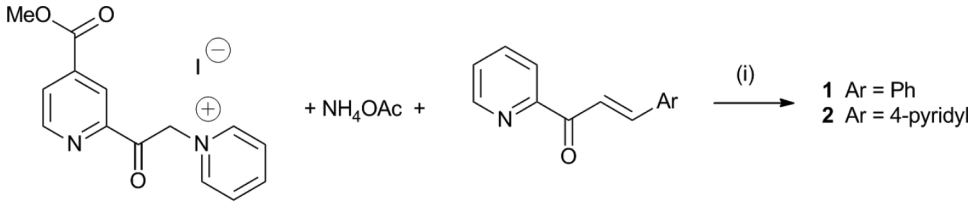

Fig. 1. ORTEP representation of the structure of **1** (ellipsoids plotted at 50% probability level). Selected bond parameters: N1–C1 = 1.342(2), N1–C5 = 1.3386(19), N2–C6 = 1.3415(18), N2–C10 = 1.3412(17), N3–C11 = 1.3463(17), N3–C15 = 1.3295(19), C13–C22 = 1.4993(19), O1–C22 = 1.2052(18), C22–O2 = 1.3309(18), O2–C23 = 1.4524(18) Å; C5–N1–C1 = 117.26(13), C6–N2–C10 = 117.72(12), C15–N3–C11 = 117.80(12), O1–C22–O2 = 124.63(13), O1–C22–C13 = 124.21(13), O2–C22–C13 = 111.15(12), C22–O2–C23 = 117.15(12)°.

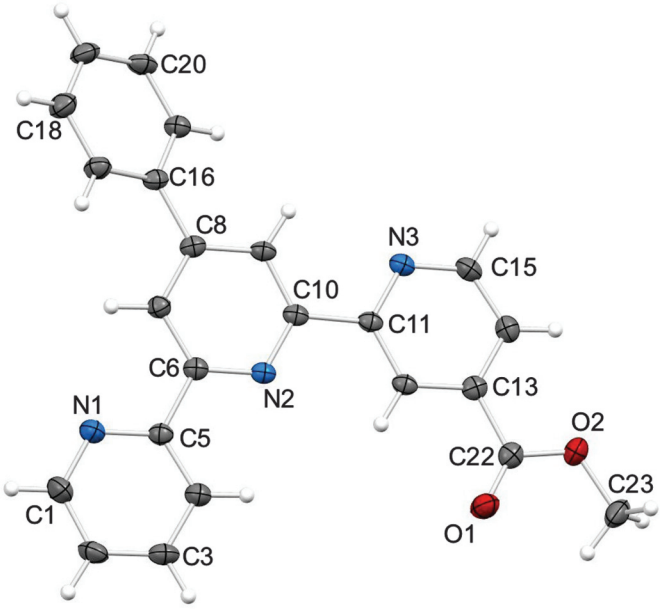

Scheme 3. Synthesis of phosphonate **4**. Conditions: (*i*) $[Pd(PPh_3)_4]$, NEt_3, $HP(O)(OEt)_2$, MeCN, 140 °C, 30 min.

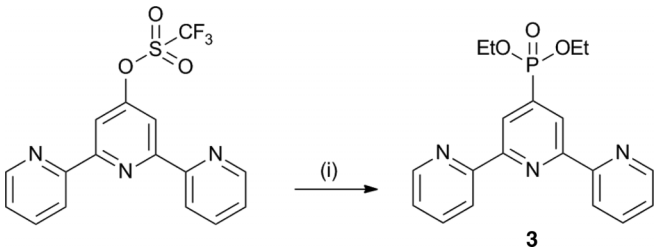

um(II) centre bound by the bis(chelating) donor sets of pytpy and ligand **4**. Despite attempts, X-ray-quality single crystals of the other ruthenium(II) complexes were not obtained.

Absorption and emission spectroscopic properties

The absorption spectra of MeCN solutions of the complexes are shown in Fig. 4. Each exhibits a series of high-energy bands arising from ligand-based, spin-allowed transitions and a broad MLCT band in the visible region. The values of λ_{max} for the MLCT absorptions (485–491 nm, see Experimental section) compare with 488 nm for both $[Ru(Phtpy)_2][PF_6]_2$[26] and $[Ru(pytpy)_2][PF_6]_2$.[28] The spectra for $[Ru(Phtpy)(\mathbf{4})][PF_6]_2$ and $[Ru(pytpy)(\mathbf{4})][PF_6]_2$ are similar to one another and to those of the homoleptic complexes

Scheme 4. Structures of the heteroleptic complex cations prepared as hexafluoridophosphate salts.

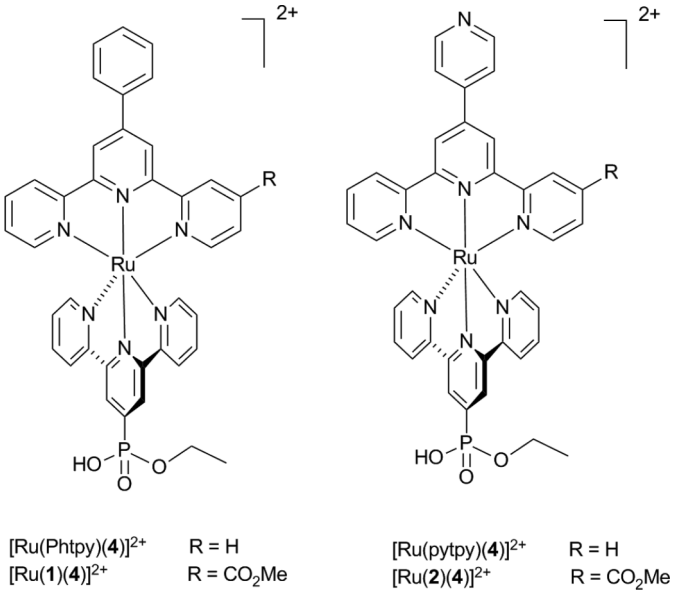

Fig. 2. Aromatic region of the 400 HMz ^{1}H NMR spectrum of $[Ru(Phtpy)(\mathbf{4})][PF_6]_2$. See Scheme 1 for ring labelling.

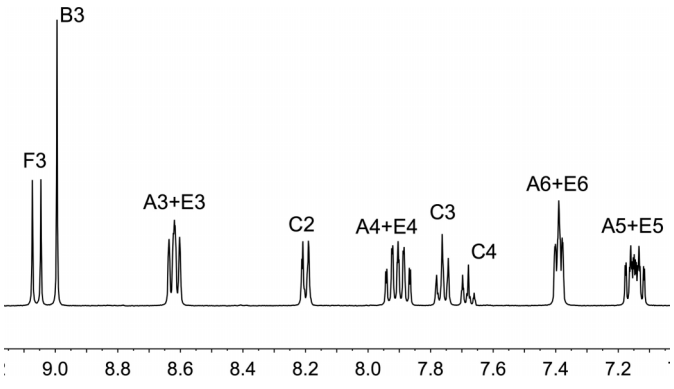

Fig. 3. Aromatic region of the 500 HMz ^{1}H NMR spectrum of $[Ru(\mathbf{2})(\mathbf{4})][PF_6]_2$. See Scheme 1 for ring labelling.

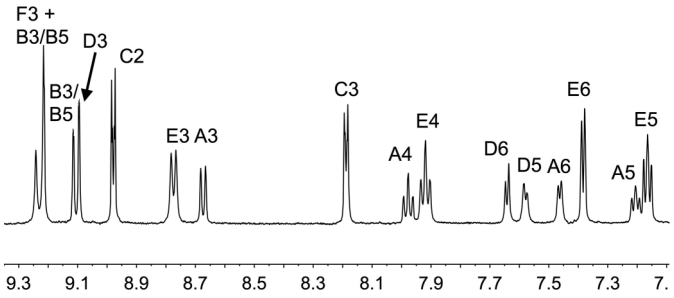

Fig. 4. Absorption spectra of MeCN solutions of [Ru(Phtpy)(**4**)][PF_6]$_2$, [Ru(pytpy)(**4**)][PF_6]$_2$, [Ru(**1**)(**4**)][PF_6]$_2$, and [Ru(**2**)(**4**)][PF_6]$_2$. See Experimental section for concentrations.

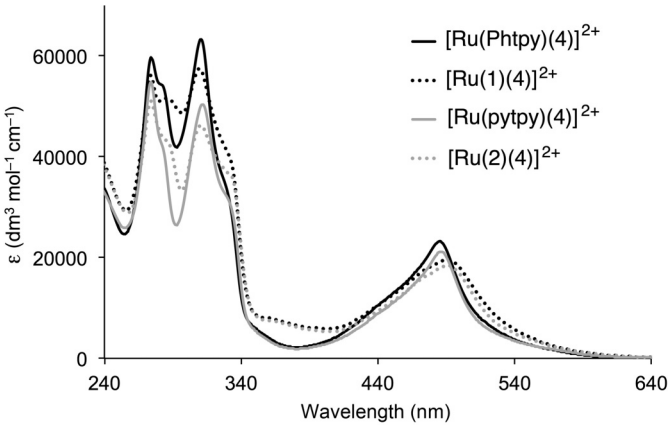

[Ru(Phtpy)$_2$][PF_6]$_2$[26] and [Ru(pytpy)$_2$][PF_6]$_2$.[28] The introduction of the methyl ester substituent leads to a change in the appearance of the absorption maxima (Fig. 4), the trend being the same on going from [Ru(Phtpy)(**4**)][PF_6]$_2$ to [Ru(**1**)(**4**)][PF_6]$_2$, and from [Ru(pytpy)(**4**)][PF_6]$_2$ to [Ru(**2**)(**4**)][PF_6]$_2$. The small red shift in the MLCT band upon introduction of the CO_2Me group is consistent with that observed on going from [Ru(ttpy)$_2$]$^{2+}$ to [Ru(4-MeO_2Cttpy)$_2$]$^{2+}$ (ttpy = 4′-tolyl-2,2′:6′,2″-terpyridine; 4-MeO_2Cttpy = 4-carboxymethyl-4′-tolyl-2,2′:6′,2″-terpyridine).[25]

Excitation into the MLCT band of each of [Ru(Phtpy)(**4**)][PF_6]$_2$ and [Ru(**1**)(**4**)][PF_6]$_2$ (in degassed MeCN at room temperature) gives rise to a weak emission at 647 and 665 nm, respectively, with a quantum yield below the detection limit of the instrument (<1%).

Electrochemical properties

The complexes are electrochemically active and cyclic voltammetric data are given in Table 1. The reversible oxidation observed for each complex arises from the Ru^{2+}/Ru^{3+} couple. For the parent [Ru(tpy)$_2$]$^{2+}$, this process occurs at +0.918 V,[26] and introducing electron-donating phenyl groups shifts it to lower potential (+0.895 V in [Ru(Phtpy)$_2$][PF_6]$_2$).[26] Replacing one phenyl substituent by the electron-withdrawing phosphonic ester group shifts the oxidation to +0.93 V (Table 1). A similar trend is seen on comparing the Ru^{2+}/Ru^{3+} potential in [Ru(pytpy)$_2$][PF_6]$_2$ (+0.95 V)[28] with that in [Ru(pytpy)(**4**)][PF_6]$_2$ (+1.01 V). Introduction of the methyl ester unit results in a 0.03 V shift to more positive potential on going from [Ru(Phtpy)(**4**)][PF_6]$_2$ to [Ru(**1**)(**4**)][PF_6]$_2$ or from [Ru(pytpy)(**4**)][PF_6]$_2$ to [Ru(**2**)(**4**)][PF_6]$_2$. This is consistent with the trend observed from [Ru(ttpy)$_2$]$^{2+}$ to [Ru(4-MeO_2Cttpy)$_2$]$^{2+}$.[25] A series of ligand-based reduction processes is observed for each complex (Table 1), consistent with expectations based on related compounds.

Conclusions

We have prepared and characterized four new heteroleptic complexes containing {Ru(tpy)$_2$} cores. One ligand contains a phosphonate ester group designed to act as an anchoring group to metal oxide surfaces. The second ligand is Phtpy or pytpy in the model systems and contains a methyl ester functionality in the second of each pair of complexes. This provides a suitable site for variable functionalization, for example, through transesterification. We plan to use the heteroleptic complexes as a starting point for development of ruthenium(II) dyes suited for sensitization of p-type semiconductors.

Table 1. Cyclic voltammetric data for the ruthenium(II) complexes with respect to Fc/Fc$^+$ in MeCN solutions with [^{t}Bu$_4$N][PF_6] as supporting electrolyte and a scan rate of 0.1 V s^{-1} (ir, irreversible; qr, quasi-reversible).

Complex	$E_{1/2}^{ox}$ (V)	$E_{1/2}^{red}$ (V)
[Ru(Phtpy)(**4**)][PF_6]$_2$	+0.93	−1.68, −1.93^{qr}
[Ru(**1**)(**4**)][PF_6]$_2$	+0.96	−1.49, −1.90, −2.23^{ir}
[Ru(pytpy)(**4**)][PF_6]$_2$	+1.01	−1.57, −2.00^{ir}
[Ru(**2**)(**4**)][PF_6]$_2$	+1.04	−1.43, −1.85

Supplementary material

CCDC 983369 contains the supplementary crystallographic data for this paper. These data can be obtained, free of charge, via http://www.ccdc.cam.ac.uk/products/csd/request/ (or from the Cambridge Crystallographic Data Centre, 12 Union Road, Cambridge CB2 1EZ, UK (fax: 44-1223-336033 or e-mail: deposit@ccdc.cam.ac.uk)).

Acknowledgements

We thank the Swiss National Science Foundation, the European Research Council (advanced grant 267816 LiLo), and the University of Basel for financial support. Sven Brauchli and Dr. Heinz Nadig are acknowledged for recording mass spectra. Angelo Lanzilotto is thanked for assistance with absorption spectroscopic measurements.

References

(1) See for example: (a) Sauvage, J.-P.; Collin, J.-P.; Chambron, J. C.; Guillerez, S.; Coudret, C.; Balzani, V.; Barigelletti, F.; De Cola, L.; Flamigni, L. *Chem. Rev.* **1994**, *94*, 993. doi:10.1021/cr00028a006; (b) Constable, E. C. *Chem. Commun.* **1997**, 1073. doi:10.1039/A605102B; (c) Baranoff, E.; Collin, J.-P.; Flamigni, L.; Sauvage, J.-P. *Chem. Soc. Rev.* **2004**, *33*, 147. doi:10.1039/b308983e; (d) Andres, P. R.; Schubert, U. S. *Adv. Mater.* **2004**, *16*, 1043. doi:10.1002/adma.200306518.
(2) Kröhnke, F. *Synthesis* **1976**, 1. doi:10.1055/s-1976-23941.
(3) Campagna, S.; Puntoriero, F.; Nastasi, F.; Bergamini, G.; Balzani, V. *Topic Curr. Chem.* **2007**, *280*, 117. doi:10.1007/128_2007_133.
(4) Maestri, M.; Armaroli, N.; Balzani, V.; Constable, E. C.; Cargil Thompson, A. M. W. *Inorg. Chem.* **1995**, *34*, 2759. doi:10.1021/ic00114a039.
(5) Grätzel, M. *Inorg. Chem.* **2005**, *44*, 6841. doi:10.1021/ic0508371.
(6) Bozic-Weber, B.; Constable, E. C.; Housecroft, C. E. *Coord. Chem. Rev.* **2013**, *257*, 3089. doi:10.1016/j.ccr.2013.05.019.
(7) Bozic-Weber, B.; Brauchli, S.; Constable, E. C.; Fürer, S. O.; Housecroft, C. E.; Wright, I. A. *Phys. Chem. Chem. Phys.* **2013**, *15*, 4500. doi:10.1039/C3CP50562F.
(8) See for example: (a) Fan, S.-Q.; Kim, C.; Fang, B.; Liao, K.-X.; Yang, G.-J.; Li, C.-J.; Kim, J.-J.; Ko, J. *J. Phys. Chem. C.* **2011**, *115*, 7747. doi:10.1021/jp200700e; (b) Wang, S.-W.; Wu, K.-L.; Ghadiri, E.; Lobello, M. G.; Ho, S.-T.; Chi, Y.; Moser, J.-E.; De Angelis, F.; Grätzel, M.; Nazeeruddin, M. K. *Chem. Sci.*, **2013**, *4*, 2423. doi:10.1039/c3sc50399b; (c) Nguyen, L. H.; Mulmudi, H. K.; Sabba, D.; Kulkarni, S. A.; Batabyal, S. K.; Nonomura, K.; Grätzel, M.; Mhaisalkar, S. G. *Phys. Chem. Chem. Phys.* **2012**, *14*, 16182. doi:10.1039/C2CP42959D.
(9) He, J.; Lindström, H.; Hagfeldt, A.; Lindquist, S.-E. *Solar Ener. Mater. Solar Cells* **2000**, *62*, 265. doi:10.1016/S0927-0248(99)00168-3.
(10) Mishra, A.; Fischer, M. K. R.; Bäuerle, P. *Angew. Chem. Int. Ed.* **2009**, *48*, 2474. doi:10.1002/anie.200804709.
(11) Pellegrin, Y.; Le Pleux, L.; Blart, E.; Renaud, A.; Chavillon, B.; Szuwarski, N.; Boujtita, M.; Cario, L.; Jobic, S.; Jacquemin, D.; Odobel, F. *J. Photochem. Photobiol. A* **2011**, *219*, 235. doi:10.1016/j.jphotochem.2011.02.025.
(12) Constable, E. C.; Homes, J. M. *J. Organomet. Chem.* **1986**, *301*, 203. doi:10.1016/0022-328X(86)80011-0.
(13) Reveco, P.; Cherry, W. R.; Medley, J.; Garber, A.; Gale, R. J.; Selbin, J. *Inorg. Chem.* **1986**, *25*, 1842. doi:10.1021/ic00231a025.
(14) Ji, Z.; Natu, G.; Huang, Z.; Kokhan, O.; Zhang, X.; Wu, Y. *J. Phys. Chem. C* **2012**, *116*, 16854. doi:10.1021/jp303909x.
(15) Ji, Z.; Wu, Y. *J. Phys. Chem. C* **2013**, *117*, 18315. doi:10.1021/jp405659m.
(16) Eryazici, I.; Moorefield, C. N.; Durmus, S.; Newkome, G. R. *J. Org. Chem.* **2006**, *71*, 1009. doi:10.1021/jo052036l.
(17) Zhao, L.-X.; Kim, T. S.; Ahn, S.-H.; Kim, T.-H.; Kim, E.; Cho, W.-J.; Choi, H.; Lee, C.-S.; Kim, J.-A.; Jeong, T. C.; Chang, C.; Lee, E.-S. *Bioorg. Med. Chem. Lett.* **2001**, *11*, 2659. doi:10.1016/S0960-894X(01)00531-5.
(18) Wang, J.; Hanan, G. S. *Synlett* **2005**, *8*, 1251. doi:10.1055/s-2005-868481.
(19) Potts, K. T.; Konwar, D. *J. Org. Chem.* **1991**, *56*, 4815. doi:10.1021/jo00015a050.
(20) Zakeeruddin, S. M.; Nazeeruddin, M. K.; Pechy, P.; Rotzinger, F. P.; Humphry-Baker, R.; Kalyanasundaram, K.; Grätzel, M. *Inorg. Chem.* **1997**, *36*, 5937. doi:10.1021/ic970008i.

(21) *APEX2, Version 2 User Manual, M86-E01078*; Bruker Analytical X-ray Systems, Inc.: Madison, WI, 2006.
(22) Sheldrick, G. M. *Acta Cryst.* **2008**, *A64*, 112. doi:10.1107/S0108767307043930.
(23) Bruno, I. J.; Cole, J. C.; Edgington, P. R.; Kessler, M. K.; Macrae, C. F.; McCabe, P.; Pearson, J.; Taylor, R. *Acta Cryst.* **2002**, *B58*, 389. doi:10.1107/S0108768102003324.
(24) Macrae, C. F.; Bruno, I. J.; Chisholm, J. A.; Edgington, P. R.; McCabe, P.; Pidcock, E.; Rodriguez-Monge, L.; Taylor, R.; van de Streek, J.; Wood, P. A. *J. Appl. Cryst.* **2008**, *41*, 466. doi:10.1107/S0021889807067908.
(25) Mikel, C.; Potvin, P. G. *Polyhedron* **2002**, *21*, 49. doi:10.1016/S0277-5387(01)00959-7.
(26) Constable, E. C.; Cargill Thompson, A. M. W.; Tocher, D. A.; Daniels, M. A. M. *New J. Chem.* **1992**, *16*, 855.
(27) Zhong, D. K.; Zhao, S.; Polyansky, D. E.; Fujita, E. *J. Catal.* **2013**, *307*, 140. doi:10.1016/j.jcat.2013.07.018.
(28) Constable, E. C.; Cargill Thompson, A. M. W. *J. Chem. Soc., Dalton Trans.* **1994**, 1409. doi:10.1039/DT9940001409.